International Journal of Thermophysics, Vol. 23, No. 6, November 2002 (© 2002)

Compressed Liquid and Supercritical Densities of 1,1,1,2,3,3,3-Heptafluoropropane (R227ea)

E. C. Ihmels,[1] S. Horstmann,[2] K. Fischer,[2,3] G. Scalabrin,[4] and J. Gmehling[1]

Received January 22, 2002

Densities of 1,1,1,2,3,3,3-heptafluoropropane (R227ea) have been measured with a computer-controlled high-temperature high-pressure vibrating-tube densimeter system (DMA-HDT) in the sub- and supercritical states. The densities were measured at temperatures from 278 to 473 K and pressures up to 30 MPa (overall 257 data points), whereby a density range between 285 and 1588 $kg \cdot m^{-3}$ was covered. The uncertainty in the density measurement was estimated to be better than $\pm 0.2\ kg \cdot m^{-3}$. The experimental data of R227ea were correlated with a virial-type equation of state (EoS) and compared with published data. A comparison is also made with a recent wide-range dedicated equation of state for R227ea.

KEY WORDS: density; equation of state; R227ea; vibrating tube densimeter.

1. INTRODUCTION

A reliable knowledge of the $P\rho T$ behavior of pure compounds and mixtures is of great interest in many fields of research as well as in industrial practice. The densities of fluids as a function of temperature, pressure, and composition are particularly important for the design of industrial plants, pipelines, and pumps. Furthermore, accurate experimental density data are the basis for the development of new correlation equations and improved equations of state (EoS). Information about the $P\rho T$ behavior and ideal gas heat capacities allow the calculation of phase equilibria and other

[1] Department of Industrial Chemistry, University of Oldenburg, P.O. Box 2503, D-26111 Oldenburg, Germany.
[2] Laboratory for Thermophysical Properties (LTP GmbH), Institute at the University of Oldenburg, P.O. Box 2503, D-26111 Oldenburg, Germany.
[3] To whom correspondence should be addressed. E-mail: Fischer@tech.chem.uni-oldenburg.de
[4] Dipartimento di Fisica Tecnica, Università di Padova, via Venezia 1, I-35131 Padova, Italy.

0195-928X/02/1100-1571/0 © 2002 Plenum Publishing Corporation

thermodynamic properties such as enthalpies, entropies, heat capacities, and heats of vaporization at given conditions (temperature, pressure, and composition). These data are needed for solving material and energy balance equations required for the design and optimization of chemical processes.

Since the beginning of 2001 the use of any chlorofluorocarbons (CFCs) has been prohibited in Europe because of their threat to the ozone layer [1]. Also, the use of some hydrochlorofluorocarbons (HCFCs) was forbidden and the ban will be extended to further HCFCs in the near future. An alternative group of refrigerants includes the hydrofluorocarbons (HFCs) such as 1,1,1,2,3,3,3-heptafluoropropane (R227ea). They have been developed as a group of zero ozone-depletion refrigerants. The greenhouse gas potential of HFCs is in most cases much lower than that for HCFCs and CFCs. Since the beginning of the 1990s, R227ea has been produced in large scale and used as a propellant for medical aerosols, particularly for asthma sprays, and for fire extinguishers.

For R227ea only a few experimental density data in the vapor, compressed liquid, and supercritical states are available in the literature [2–6]. Due to the limited temperature and pressure range covered by these data, experimental investigations were performed here by means of a vibrating tube densimeter. The data are presented in comparison to correlated values using a virial-type EoS and to the experimental data of other authors.

2. EXPERIMENTAL

1,1,1,2,3,3,3-heptafluoropropane (R227ea, Solkane 227 pharma from Solvay, C_3HF_7, $M = 170.03\ g/mol$, CAS-RN 431-89-0) was supplied without inert components (e.g., air) and used without further purification. The purity (> 99.9 mass%) was checked by gas chromatography.

A computer-operated vibrating tube densimeter system for high temperatures and pressures (temperatures from 273 to 623 K and pressures up to 40 MPa) was used for the measurement of the density data for R227ea. The automated equipment can be used for the determination of densities in the sub- and supercritical states. With this apparatus, a large number of data points can be obtained in a rather short time with a minimum amount of manual effort. A temperature and pressure program can be used to obtain a complete $P\rho T$ field for the desired component. The data of several liquids and liquefied gases (toluene, carbon dioxide, carbonyl sulfide, hydrogen sulfide, sulfur hexafluoride, and dinitrogen monoxide) have already been published [7, 8]. Comparisons with reference EoS for toluene,

CO_2, and SF_6 demonstrated the high accuracy and suitability of this measurement system.

The apparatus and procedure of the measurements were described in detail by Ihmels and Gmehling [7]. A prototype of a high-pressure high-temperature vibrating tube densimeter (DMA-HDT) is the essential part of the experimental setup. The temperature is measured using a Pt100 resistance thermometer and the pressure is monitored by means of a calibrated external pressure sensor (Model PDCR 911, pressure range 60 MPa, Druck). The density values are obtained from the periods of oscillation of the vibrating tube. For the calibration the period of oscillation at zero pressure and for the two reference substances water and butane was used in the investigated temperature and pressure range. The reference densities were calculated using the reference EoS from Pruß and Wagner [9, 10] for water and the EoS from Younglove and Ely [11] for butane. The measured data are subject to experimental errors. The uncertainty of the temperature measurement is estimated to be ± 0.03 K, and the measurement of pressure has an estimated uncertainty of ± 6 kPa. A maximum error of $\pm 0.2\ \mathrm{kg \cdot m^{-3}}$ exists for density measurements in the temperature and pressure range covered (278 to 473 K, 1 to 40 MPa). For the measured densities between 300 and 1500 $\mathrm{kg \cdot m^{-3}}$ this leads to relative errors between $\pm 0.07\%$ and $\pm 0.015\%$. The estimated errors are based on the comparison of experimental data for reference substances (other than those used for calibration) and established literature data [7, 8]. Because of the strong pressure dependence of the densities near the critical point, higher deviations are obtained in this region. With an uncertainty in pressure of ± 6 kPa, a maximum error in density of about $\pm 0.5\%$ in the supercritical region ($T > T_c$) near the critical pressure and of about $\pm 2\%$ in the region near the critical point is estimated.

3. RESULTS AND DISCUSSION

In this work, the densities of R227ea were measured from 278 to 473 K and from 0.9 up to 30 MPa. The results (257 data points) are listed in Table I and presented graphically in Fig. 1. In the compressed liquid state, densities of R227ea have already been measured from 205 K to the critical temperature, and up to pressures of 51 MPa [2, 3, 5]. In the supercritical region, data are available up to 423 K and 50 MPa [4, 5]. With the new measurements the temperature range was extended up to 473 K. $P\rho T$ data have also been published for the vapor phase [5, 6]. The range of all available density data from the different references are represented in Figs. 2 and 3.

Table I. Experimental Densities of 1,1,1,2,3,3,3-Heptafluoropropane (R227ea)

T (K)	P (MPa)	ρ (kg·m^{-3})	T (K)	P (MPa)	ρ (kg·m^{-3})
278.24	0.916	1470.85	308.25	4.979	1382.27
278.24	4.982	1492.63	308.25	9.982	1416.79
278.24	9.984	1516.00	308.25	14.984	1445.23
278.24	14.985	1536.61	308.25	19.983	1469.69
278.24	19.988	1555.17	308.25	24.986	1491.33
278.24	24.990	1572.14	308.25	29.987	1510.83
278.24	29.985	1587.77	313.15	1.433	1329.64
283.24	1.003	1452.30	313.15	4.979	1362.70
283.24	4.984	1475.19	313.15	9.981	1399.75
283.24	9.984	1500.02	313.15	14.984	1429.81
283.24	14.985	1521.70	313.15	19.983	1455.44
283.24	19.987	1541.12	313.15	24.987	1477.98
283.24	24.987	1558.76	313.15	29.996	1498.18
283.24	29.990	1574.99	318.15	5.022	1342.85
288.24	1.055	1433.09	318.15	9.985	1382.09
288.24	4.983	1457.44	318.15	14.989	1413.96
288.24	9.983	1483.84	318.15	19.982	1440.82
288.24	14.983	1506.68	318.15	24.988	1464.33
288.24	19.985	1526.99	318.15	29.988	1485.30
288.24	24.992	1545.36	323.15	5.020	1320.64
288.24	29.987	1562.19	323.15	9.978	1364.02
293.25	1.114	1413.40	323.15	14.994	1397.91
293.25	4.979	1439.29	323.15	20.008	1426.23
293.25	9.984	1467.44	323.15	24.989	1450.61
293.24	14.985	1491.54	323.15	29.994	1472.40
293.25	19.985	1512.80	328.15	5.022	1298.86
293.24	24.986	1531.93	328.15	9.980	1345.69
293.25	29.992	1549.38	328.15	14.980	1381.58
298.25	1.180	1393.16	328.15	19.983	1411.28
298.25	4.985	1420.77	328.15	24.991	1436.86
298.25	9.986	1450.82	328.15	29.979	1459.38
298.25	14.983	1476.25	333.15	1.914	1230.58
298.25	19.986	1498.52	333.15	4.978	1275.61
298.25	24.987	1518.44	333.15	9.980	1327.14
298.25	29.989	1536.56	333.15	14.986	1365.25
303.25	1.255	1372.36	333.15	19.986	1396.42
303.25	4.978	1401.74	333.15	24.983	1423.06
303.25	9.984	1433.95	333.15	29.987	1446.50
303.25	14.985	1460.82	338.14	2.061	1202.92
303.25	19.987	1484.16	338.14	4.980	1251.69
303.25	24.987	1504.92	338.14	9.980	1307.95
303.25	30.019	1523.83	338.14	14.986	1348.59
308.25	1.296	1350.55	338.14	19.986	1381.41

Table I. *(Continued)*

T (K)	P (MPa)	ρ (kg·m^{-3})	T (K)	P (MPa)	ρ (kg·m^{-3})
338.14	24.984	1409.22	368.13	29.993	1355.36
338.14	29.989	1433.54	373.12	3.521	949.52
343.14	2.229	1173.81	373.13	4.978	1037.05
343.14	4.982	1226.65	373.13	9.985	1160.32
343.14	9.980	1287.88	373.13	14.985	1226.08
343.14	14.981	1331.76	373.13	19.988	1273.31
343.14	19.987	1366.29	373.13	24.985	1310.98
343.14	24.987	1395.32	373.13	29.993	1342.35
343.14	29.984	1420.52	378.12	5.024	996.61
348.13	2.405	1142.75	378.13	9.976	1136.84
348.14	4.981	1200.23	378.12	14.980	1207.69
348.14	9.982	1268.02	378.12	19.983	1257.41
348.14	14.981	1314.73	378.12	24.993	1296.87
348.14	19.983	1351.05	378.12	29.989	1329.27
348.14	24.984	1381.34	383.12	5.023	948.71
348.14	29.985	1407.51	383.12	9.987	1113.06
353.13	2.597	1109.58	383.12	14.985	1189.19
353.13	4.979	1172.21	383.12	19.987	1241.58
353.13	9.980	1247.57	383.12	24.991	1282.61
353.13	14.980	1297.46	383.12	29.991	1316.25
353.14	19.983	1335.71	388.11	5.023	893.37
353.13	24.984	1367.34	388.12	9.978	1088.27
353.13	29.985	1394.49	388.12	14.980	1170.38
358.13	2.805	1074.04	388.12	19.982	1225.58
358.13	5.023	1143.42	388.12	24.983	1268.15
358.13	10.023	1227.12	388.12	29.992	1303.22
358.13	14.986	1279.96	393.11	5.020	828.75
358.13	19.980	1320.25	393.12	9.983	1063.00
358.13	24.990	1353.32	393.12	14.984	1151.47
358.14	29.984	1381.46	393.12	19.982	1209.56
363.13	3.028	1035.55	393.12	24.983	1253.59
363.13	4.978	1110.23	393.12	29.983	1290.18
363.13	9.988	1205.13	398.11	5.024	754.15
363.13	14.988	1262.21	398.12	9.979	1037.00
363.13	19.983	1304.69	398.12	14.980	1132.27
363.13	24.992	1339.27	398.12	19.986	1193.46
363.13	29.992	1368.46	398.12	24.984	1239.38
368.12	3.268	994.09	398.12	29.983	1277.19
368.13	4.989	1075.74	403.10	5.024	673.74
368.13	9.982	1182.97	403.11	9.983	1010.47
368.13	14.981	1244.15	403.11	14.979	1112.93
368.13	19.987	1289.06	403.11	19.981	1177.31
368.13	24.979	1325.08	403.11	24.992	1225.23

Table I. *(Continued)*

T (K)	P (MPa)	ρ (kg·m^{-3})	T (K)	P (MPa)	ρ (kg·m^{-3})
403.11	29.986	1264.28	443.11	5.024	354.25
408.10	5.024	597.48	443.10	9.982	786.06
408.11	9.983	983.24	443.10	14.984	955.13
408.11	14.983	1093.49	443.10	19.981	1047.90
408.11	19.985	1161.17	443.10	24.982	1112.03
408.11	24.986	1210.98	443.10	29.992	1161.52
408.11	29.994	1251.46	448.10	5.017	338.51
413.11	5.023	534.68	448.10	9.980	758.88
413.11	10.023	956.84	448.10	14.982	935.64
413.11	15.021	1074.53	448.10	19.982	1031.91
413.11	19.982	1144.91	448.10	24.991	1098.18
413.11	24.983	1196.73	448.10	29.983	1148.97
413.11	29.984	1238.61	453.10	5.022	325.91
418.11	5.024	485.45	453.10	9.981	732.97
418.11	9.983	927.35	453.10	14.982	916.25
418.11	14.986	1054.21	453.10	19.982	1016.06
418.11	19.982	1128.69	453.10	24.984	1084.37
418.11	24.983	1182.52	453.10	29.983	1136.56
418.11	29.980	1224.97	458.10	5.023	314.26
423.11	5.024	447.27	458.10	9.983	707.99
423.11	9.979	898.78	458.10	14.982	897.08
423.11	14.981	1034.31	458.10	19.983	1000.33
423.11	19.983	1112.47	458.10	24.984	1070.68
423.11	24.990	1168.36	458.10	29.985	1124.23
423.11	29.988	1212.06	463.10	5.021	303.52
428.10	5.024	416.97	463.10	9.980	684.14
428.10	9.976	870.10	463.10	14.981	878.23
428.11	14.977	1014.40	463.10	19.986	984.70
428.11	19.980	1096.21	463.10	24.982	1057.04
428.11	24.984	1154.19	463.10	29.984	1111.96
428.11	29.991	1199.42	468.10	5.024	294.24
433.11	5.024	392.35	468.10	9.999	662.43
433.11	9.984	841.95	468.10	15.022	860.83
433.11	14.987	994.77	468.10	20.018	969.89
433.11	19.984	1080.09	468.10	24.980	1043.50
433.11	24.985	1140.07	468.10	29.986	1099.82
433.11	29.988	1186.74	473.10	5.024	285.44
438.10	5.024	371.77	473.10	9.986	640.32
438.10	9.984	813.80	473.10	14.983	841.49
438.10	14.981	974.78	473.10	19.981	954.02
438.10	19.987	1064.03	473.10	24.990	1030.23
438.10	24.983	1126.03	473.10	29.992	1087.84
438.10	29.982	1174.05			

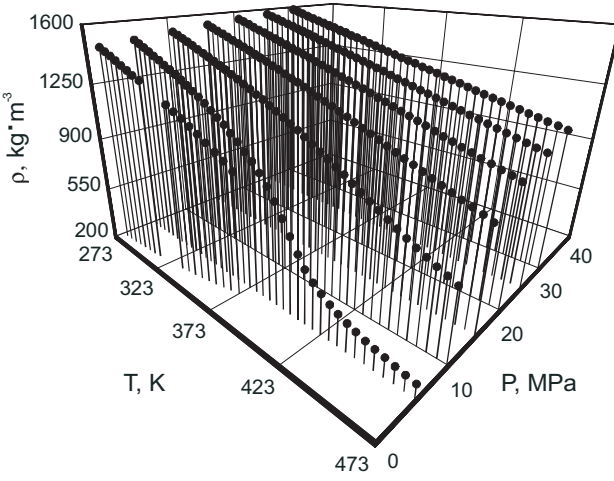

Fig. 1. Experimental densities of 1,1,1,2,3,3,3-heptafluoropropane (R227ea).

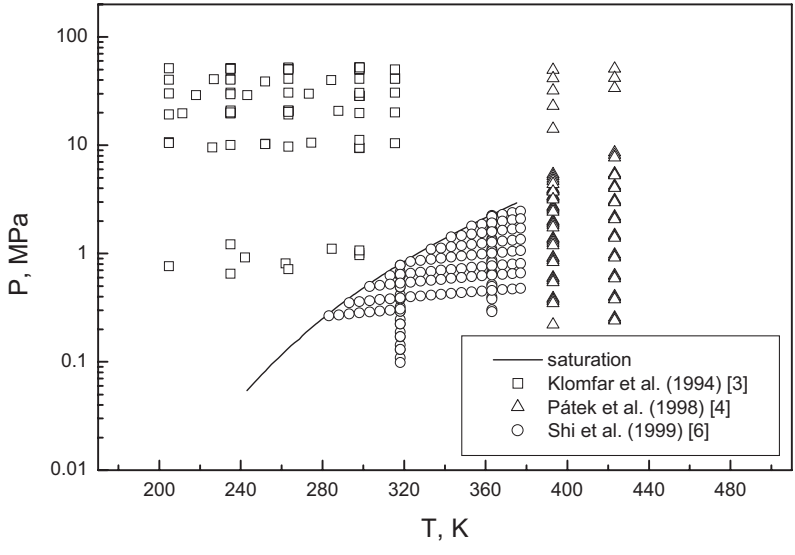

Fig. 2. *PT* diagram of the experimental density data for 1,1,1,2,3,3,3-heptafluoropropane (R227ea) from Klomfar et al. [3], Pátek et al. [4], and Shi et al. [6].

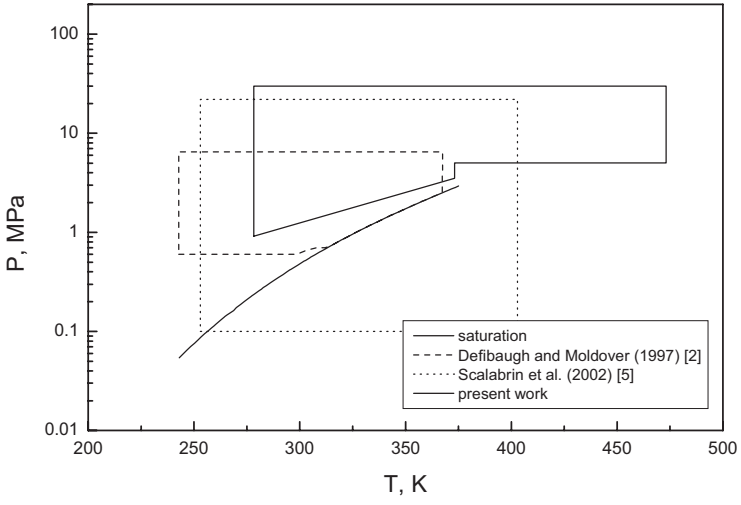

Fig. 3. *PT* range of the experimental data for 1,1,1,2,3,3,3-heptafluoropropane (R227ea) covered by the experimental data of Defibaugh and Moldover [2] and Scalabrin et al. [5].

A virial-type EoS

$$P = T\rho[R + B\rho + C\rho^2 + D\rho^3 + E\rho^4 + F\rho^5] \tag{1}$$

with the following temperature dependent functions

$$B = a_1 - \frac{a_2}{T} - \frac{a_3}{T^2} - \frac{a_4}{T^3} - \frac{a_5}{T^4} \tag{2}$$

$$C = a_6 + \frac{a_7}{T} + \frac{a_8}{T^2} \tag{3}$$

$$D = a_9 + \frac{a_{10}}{T} \tag{4}$$

$$E = a_{11} + \frac{a_{12}}{T} \tag{5}$$

and

$$F = \frac{a_{13}}{T} \tag{6}$$

Table II. Parameters for the Virial Equation for 1,1,1,2,3,3,3-Heptafluoropropane (R227ea): Temperature, Pressure and Density Range, EoS Parameters and Statistical Values, Units: K, MPa, and $mol \cdot L^{-1}$

T_{min}	278.2	a_1	0.0038995467
T_{max}	473.1	a_2	2.9150189
P_{min}	0.92	a_3	−227.01468
P_{max}	30.02	a_4	1634.4828
ρ_{min}	1.68	a_5	−41.013512
ρ_{max}	9.34	a_6	$-2.7773051 \times 10^{-5}$
data points	257	a_7	−0.022646112
RMSD (density)	0.0041	a_8	−13.960742
RMSDr (density)	0.0626	a_9	$-5.0776465 \times 10^{-5}$
bias (density)	−0.000023	a_{10}	0.095528176
RMSD (pressure)	0.0887	a_{11}	1.3543942×10^{-5}
RMSDr (pressure)	2.5859	a_{12}	−0.019939767
bias (pressure)	0.00525	a_{13}	0.0010457274

was employed for the correlation of the measured $P\rho T$ data in the sub- and supercritical states. The equation is a reduced version of the Benedict–Webb–Rubin-type Bender EoS [12]. In this equation, the exponential term of the Bender equation was omitted, so that the number of parameters was reduced from 20 to 13. The data were correlated by least squares minimization using the following objective function.

$$S = \sum_i [(\rho_{i,\,\mathrm{exp}} - \rho_{i,\,\mathrm{calc}})/\rho_{i,\,\mathrm{exp}}]^2 \tag{7}$$

In Table II, the 13 parameters of the EoS together with additional statistical values and the validity range are given. The absolute (RMSD) and relative (RMSDr) root-mean-square deviations, and the mean deviation (bias) for the density and for the pressure were calculated. In Fig. 4, the relative deviations between the experimental and the correlated values are shown. The deviations are usually within $\pm 0.2\%$. As expected, near the critical point at about $T_c = 374.88$ K and $P_c = 2.934$ MPa [13], higher deviations are observed. It is strongly recommended to use the equation parameters only within the temperature, pressure, and density ranges covered by the correlation (compressed liquid and supercritical states) and only for the calculation of $P\rho T$ properties.

Recently, an EoS for the $P\rho T$ surface has been published for R227ea [13], valid in the range of the cited references. This equation results from the combination of the ECS method and of the neural networks technique,

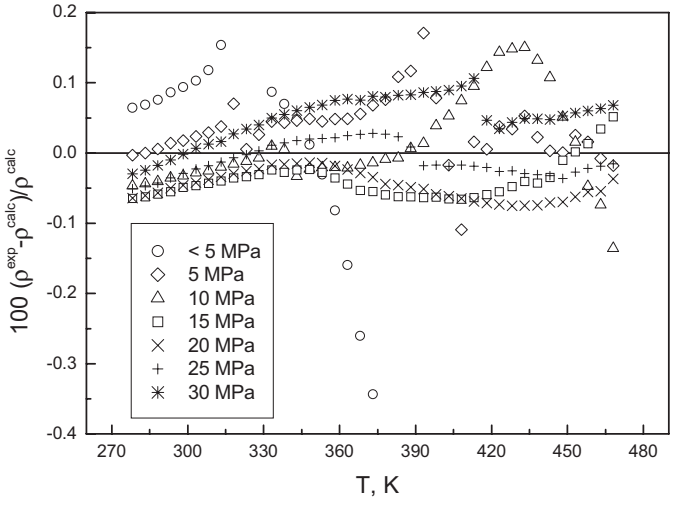

Fig. 4. Relative deviations between experimental densities from this work and the EoS correlation for 1,1,1,2,3,3,3-heptafluoropropane (R227ea).

and from now on, it will be referred to as the "ECS-NN" EoS. The cited ECS-NN EoS is a multiparameter equation of state of high accuracy dedicated to the whole thermodynamic surface of R227ea. Further more, it has a correlative nature being heuristically based solely on experimental data, and from this point of view, it is competitive with the well known Schmidt–Wagner technique for the development of a dedicated EoS in the Helmholtz energy optimized form. This EoS has been based, on purpose, on only density data, but it represents with high accuracy any thermodynamic quantity, as was demonstrated in the cited paper by Scalabrin et al. [13]. On the occasion of the publication of the new density data of the present work, that EoS has been selected as a reference one, with respect to which to check the data reliability.

For the regression of the ECS-NN EoS parameters, the density sources of Klomfar et al. [3], Pátek et al. [4], Scalabrin et al. [5], and Shi et al. [6] were used, whereas the data from Defibaugh and Moldover [2] and the data of the present work were not considered in the regression. A comprehensive validation of the cited data sources was then carried out for the present correlation, Eq. (1), and the ECS-NN EoS [13]. For the validation, only the points within the validity range of Eq. (1) were selected. The validation results are reported in Table III. In the validity range limits of these data the cited ECS-NN EoS and the present Eq. (1) reach an equivalent level of accuracy in the representation of the literature $P\rho T$ data.

Table III. Validation Results of the EoS Correlation, Eq. (1), and of the ECS-NN EoS [13] Versus Experimental $P\rho T$ Data

							EoS correlation this work			ECS-NN EoS			
Phase[a]	T Range (K)		P Range (MPa)		NPT[b]	NPR[c]	AAD (%)	Bias (%)	Max (%)	AAD (%)	Bias (%)	Max (%)	Ref.
l	243	367	0.6	6.5	1014	636	0.05	0.00	−0.24	0.13	0.13	0.24	[2]
l	205	315	0.2	51	83	19	0.25	−0.22	−0.45	0.06	0.05	0.19	[3]
l	253	374	0.2	20	6888	4835	0.16	−0.15	0.70	0.06	0.05	0.85	[5]
l	278	373	0.9	30	137	137	0.04	0.00	−0.34	0.27	0.27	0.47	[d]
sc	374	403	0.1	22	2811	2279	4.46	−4.05	−47	4.74	−4.74	−46	[5]
sc	393	423	0.2	50	81	26	4.13	3.93	14.17	0.87	0.41	4.49	[4]
sc	383	473	5	30	120	120	0.05	0.00	0.17	0.36	0.31	−0.73	[d]
Overall					**11134**	**8052**	**1.38**	**−1.22**	**−47**	**1.40**	**−1.29**	**−46**	

[a] l, liquid; sc, supercritical.
[b] NPT: total number of points.
[c] NPR: number of points falling inside the validity range of the EoS correlation.
[d] This work.

The present correlation, regressed only to the data of the present work, agree within ±0.2% with the literature data for the liquid phase. In the supercritical region, greater deviations are found with respect to the references of Pátek et al. [4] and Scalabrin et al. [5].

In the development of the ECS-NN dedicated EoS for R227ea the data of Scalabrin et al. [5] for the supercritical region were not included in the primary data sets because of their lower experimental accuracy. They have been anyway assumed for validation of the present Eq. (1) in the same region, but with expected higher deviations. The same result is also obtained with respect to the reference ECS-NN EoS; see Table III.

The deviations between the present correlation, Eq. (1), and some experimental data sources are plotted in Figs. 5 and 6 for the liquid and supercritical states, respectively. In the liquid phase, the data of Defibaugh and Moldover [2] are represented very well, while the data of Klomfar et al. [3] show greater and biased deviations. It must be recalled that, before the validation, a screening was done in which the data points outside the temperature or pressure validity range of Eq. (1) were excluded. So the validation was performed on points with temperatures or pressures very similar to those of the present work. Thus, the deviations between Eq. (1) and the literature data sources, reported in Table III and in Figs. 5 and 6, are not caused by temperature or pressure extrapolations.

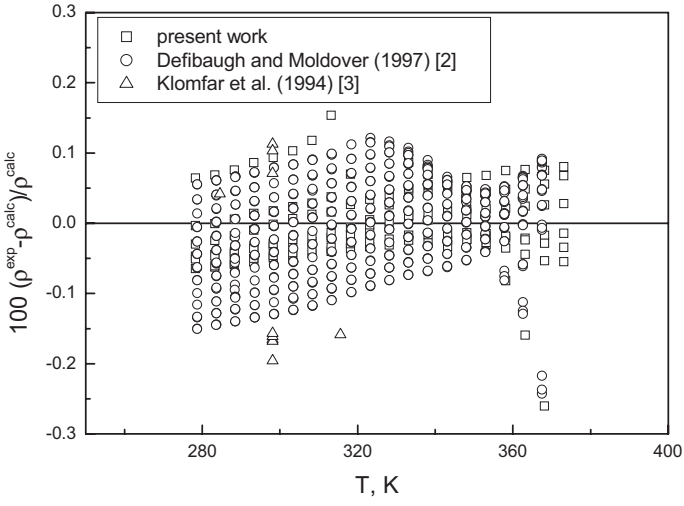

Fig. 5. Relative deviations between published experimental densities and the EoS correlation (Eq. (1)) for 1,1,1,2,3,3,3-heptafluoropropane (R227ea) (liquid phase).

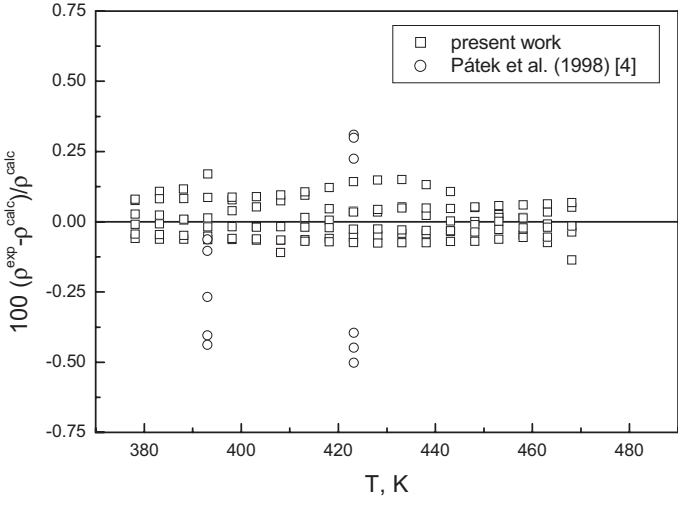

Fig. 6. Relative deviations between published experimental densities and the EoS correlation (Eq. (1)) for 1,1,1,2,3,3,3-heptafluoropropane (R227ea) (supercritical phase) (Outliers up to 4% are not shown).

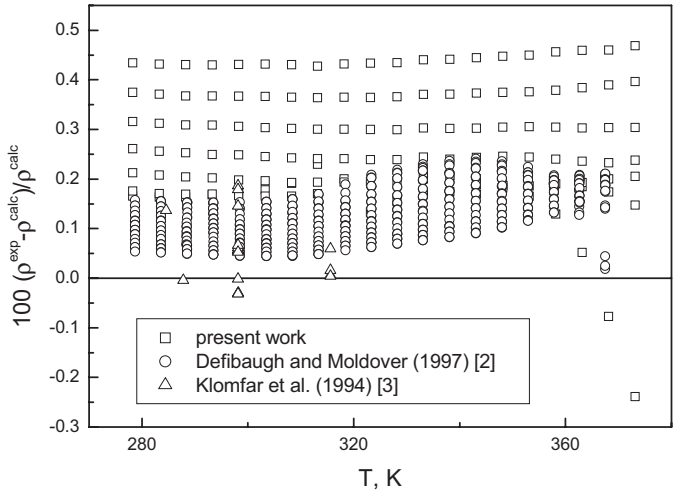

Fig. 7. Relative deviations between published experimental densities and the ECS-NN EoS for 1,1,1,2,3,3,3-heptafluoropropane (R227ea) (liquid phase).

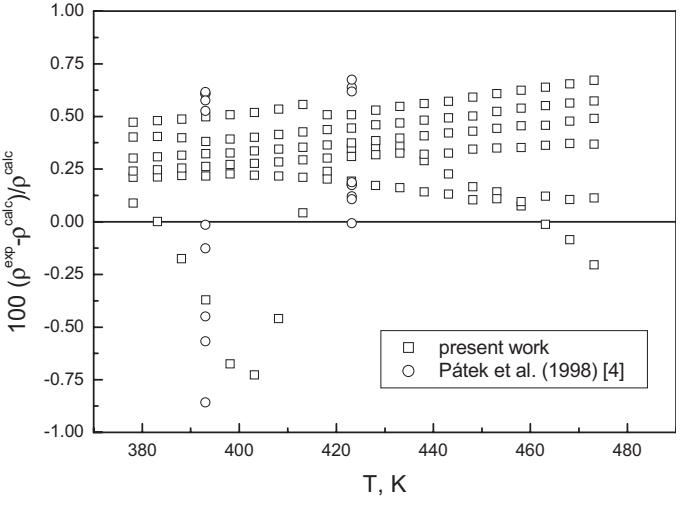

Fig. 8. Relative deviations between published densities and the ECS-NN EoS for 1,1,1,2,3,3,3-heptafluoropropane (R227ea) (supercritical phase) (Outliers up to 4.5% are not shown).

Table III shows that the ECS-NN method gives a good and balanced performance with regard to all data sets, with the exception of the data of Scalabrin et al. [5] in the supercritical phase. The average deviations of the present data set from the ECS-NN method are 0.27% in the liquid and 0.36% in the supercritical zone. The results of the ECS-NN validation are plotted in Figs. 7 and 8, respectively, for the liquid and supercritical states. In order to allow a homogeneous comparison with the correlation of the present work, the validation was conducted on the same data points selected for the validation of Eq. (1). With the exception of the present data, all of the other data sources in the supercritical region show much larger deviations than for the liquid state.

4. CONCLUSIONS

Reliable compressed liquid and supercritical densities of 1,1,1,2,3,3,3-heptafluoropropane (R227ea) were measured with the help of a computer-operated vibrating tube densimeter. For the correlation of the experimental data a virial-type EoS was employed. With the parameters given in Table II the data can be described within experimental uncertainty. By comparison with the data of other authors and also with the ECS-NN EoS, the quality of the experimental procedure was validated, so that the obtained parameters can be recommended to describe the $P\rho T$ behavior of R227ea in the covered temperature and pressure range. In the future, further results for pure components and for binary mixtures will be published. The investigation of binary mixtures will demonstrate the suitability of the measurement system for the determination of mixture data, i.e., temperature and pressure dependence of the excess volumes.

REFERENCES

1. A. H. Pischtiak, M. Pittroff, and T. Schwarze, *Characteristics, Supply and Use of the Hydrocarbons HFA 227 and HFA 134A for Medical Aerosols in the Past, Present and Future–Manufacturs Perspectives* (Solvay Fluor & Derivate GmbH, Hanover, Germany 2001)
2. D. R. Defibaugh and M. R. Moldover, *J. Chem. Eng. Data* **42**:160 (1997).
3. J. Klomfar, J. Hruby, and O. Šifner, *J. Chem. Thermodyn.* **26**:965 (1994).
4. J. Pátek, J. Klomfar, J. Pražák, and O. Šifner, *J. Chem. Thermodyn.* **30**:1159 (1998).
5. G. Scalabrin, S. Bobbo, and A. Chouai, *J. Chem. Eng. Data* **47**:258 (2002).
6. L. Shi, Y. Y. Duan, M. S. Zhu, and L. Z. Han, *J. Chem. Eng. Data* **44**:1402 (1999).
7. E. C. Ihmels and J. Gmehling, *Ind. Eng. Chem. Res.* **40**:4470 (2001).
8. E. C. Ihmels and J. Gmehling, *Int. J. Thermophys.* **23**:709 (2002).
9. A. Pruß and W. Wagner, The 1995 IAPWS–Formulation for the Thermodynamic Properties of Ordinary Water Substance for General and Scientific Use, personal communication as windows-dynamic link library (Ruhr Universität, Bochum, Germany, 1998).

10. K. Watanabe and R. B. Dooley, The International Association for the Properties of Water and Steam, Release on the IAPWS Formulation 1995 for the Thermodynamic Properties of Ordinary Water Substance for General and Scientific Use, (www.iawps.org) (Fredericia, Denmark, 1996).
11. B. A. Younglove and J. F. Ely, *J. Phys. Chem. Ref. Data* **16**:577 (1987).
12. E. Bender, *Cryogenics* **15**:667 (1975).
13. G. Scalabrin, L. Piazza, and D. Richon, *Fluid Phase Equil.* **199**:33 (2002).